83-008

PAPER NUMBER
250

CORROSION 83

The International Corrosion Forum Sponsored by the
National Association of Corrosion Engineers
Anaheim Convention Center, Anaheim, California
April 18-22, 1983

INFLUENCE OF BIOFOULING AND BIOFOULING CONTROL TECHNIQUES ON CORROSION OF COPPER-NICKEL TUBES

by

W. G. Characklis
N. Zelver
R. O. Lewis
C. H. Nelson
D. E. Dobb
G. K. Pagenkopf

Montana State University
Bozeman, MT 59717

ABSTRACT

Biofouling and corrosion of copper-nickle tubes have been observed in a laboratory sea water system. The influence of biofouling and chlorination on biofouling and corrosion have been determined. A model has been developed to aid in interpretation of the results in the context of existing literature.

INTRODUCTION

Piping systems and heat transfer surfaces in the marine environment are subject to the effects of organic and inorganic fouling. The detrimental effects of these fouling deposits include increased frictional resistance for fluid flow, increased heat transfer resistance, and, under certain conditions, an accelerating effect on corrosion of some materials.

Frictional resistance increases the power requirements for sea water pumping and reduces delivery capacity of the system. Heat transfer resistance results in a reduction in thermal efficiency of heat transfer equipment and an associated increase in energy costs.

Biofouling

Biological fouling is perhaps the least understood of all fouling processes. When a clean surface is exposed to sea water, rapid adsorption of organic molecules (primarily polysaccharides and glycoproteins) takes place (Corpe, 1973; Loeb and Neihof, 1973; Sechler and Gunderson, 1972; DePalma *et al.*, 1978). This organic adsorption is followed by the accumulation of marine bacteria (Corpe, 1973). The rates of bacterial accumulation vary on different surfaces and in different environments. Sechler and Gundersen (1972) found that bacteria may adsorb to metals at rates proportional to that with which nutrients sorb, a condition predicated by relative galvanic activity. Bryers and Characklis (1981) found, in fresh water, that biofilm accumulation increased linearly with increasing suspended biomass concentration and also increased with increasing suspended organism growth rate.

Extensive laboratory studies of the biofouling process and its effects have been conducted by Characklis and co-workers in fresh water systems (Characklis *et al.*, 1982; Characklis, 1981; Bryers and Characklis, 1981; Picologlou *et al.*, 1980; Characklis, 1980). A proposed model divides the biofouling process into three phases: (1) initial biofilm formation when the microorganisms first begin to colonize; (2) exponential accumulation of biofilm mass associated with an increase in energy losses (heat transfer resistance and frictional resistance); (3) steady-state biofouling when a plateau or asymptote in biofilm accumulation exists.

Biofouling Control Methods

Attempts to control biofouling in marine heat exchangers and piping systems have met with varying degrees of success. Chlorination and, to a lesser extent, other chemical oxidants (ozone, hydrogen peroxide, etc.) have been effectively used to combat biofouling. Copper alloys have been widely used due to their inherent "toxicity" towards many forms of marine life.

The effectiveness of chlorine in treating biofouling, including microbial slime and macrofouling organisms such as molluscs, barnacles, bryozoa, hydroids, sponges, and tunicates, has been well established (Marine Research, 1976; Bongers and O'Conner, 1977).

Chlorine can be added directly to sea water in the gaseous form or generated electrolytically. The result in both cases is the formation of hypochlorous acid which will, depending on pH, further dissociate into hypochlorite. The reaction products of chlorine are consumed in sea water not only by the organisms for which they are intended, but also by reactions with bromide, nitrogen compounds (e.g., ammonia), organic detritus and metal surfaces. All of these factors combined contribute to the chlorine demand of the sea water system and determine the relative effectiveness and cost of chlorination as a means of controlling biofouling.

Numerous researchers have reported that copper containing alloys are toxic to marine organisms (Huguenin and Ansuini, 1980; Ritter and Suitor, 1976; Nosetani *et al.*, 1979). Dexter (1974) conducted microfouling studies in warm tropical waters of the open ocean. He demonstrated that a film 50-125 μm thick could form in less than a month in warm surface waters. A continuous layer of diatoms and bacteria embedded in slime were observed on samples of 90-10 and 70-30

copper-nickel. DePalma *et al.* (1981) investigated biofouling and corrosion on titanium and copper-nickel (70-30) in sea water and observed that attached organisms produced more extracellular proteoglycan material on the titanium surface than on the copper-nickel. Furthermore, corrosion products on the copper-nickel surface were partially embedded in the biofilm and periodic sloughing of the combined biofouling and corrosion product film occurred.

Corrosion

Sea water is a very complex solution of numerous salts and dissolved gases plus suspended silt, living organisms and decaying organic matter. The corrosion of metals in sea water is affected by many factors including oxygen, salinity, pH, temperature, and biological activity.

Some metals, such as titanium, form very thin, tightly adherent protective oxide films in sea water which are essentially inert (Tracor Marine, 1978). Protective corrosion product films on copper and its alloys, by comparison, grow much more slowly and are affected significantly by thermohydrodynamic conditions.

In sea water, the corrosion product on copper-nickel alloys is predominately Cu_2O (cuprous oxide) irrespective of alloy composition (North and Pryor, 1970). Often, the basic chloride atacamite ($Cu_2(OH)_3Cl$), a bulky, green nonprotective corrosion product, forms overlaying the Cu_2O layer. A carbonate salt, malachite ($CuCO_3 \cdot Cu(OH)_2$), may form competitively with the basic chloride salt depending upon local surface pH and total inorganic carbon concentration (Bianchi and Longhi, 1973). Temperature, depth, and biological activity are the main factors influencing the total inorganic carbon concentration in sea water.

The Cu_2O corrosion product is the adherent, protective film responsible for the low corrosion rates observed on Cu-Ni alloys in unpolluted, aerated, sea water. According to Efird and Anderson (1975), the corrosion rate of 70-30 CuNi in flowing sea water (0.6 m s^{-1}) was approximately 2.0 μm yr^{-1} after 14 years exposure, but had stabilized at that value after 4 years. Efird (1975) further studied the relationship between corrosion product formation and biofouling resistance of copper base alloys. He proposed the following model to describe the process:

1. Initial formation of a protective Cu_2O film.
2. Subsequent hydrolysis of Cu_2O to a loosely adherent $Cu(OH)_2 \cdot 3CuCl_2$ film.
3. Fouling attachment to the $Cu(OH)_2 \cdot 3CuCl_2$ film.
4. Removal of the fouling organisms with the basic chloride film leaving the Cu_2O intact.

As the Cu_2O corrosion product film grows in sea water, copper ions and electrons must pass through the film to support anodic and cathodic half reactions. It has been shown experimentally (North and Pryor, 1970) that alloying additions of nickel and iron to copper improve corrosion resistance. The mechanism proposed is the incorporation of Ni and Fe ions into the highly defective p-type Cu_2O corrosion product film as "Dopants," thereby altering the defect structure. The result is a protective corrosion product film possessing relatively low electronic and ionic conductivity.

The corrosion of copper-nickel alloys in aerated, unpolluted, sea water is cathodically controlled by oxygen reduction. Dissolved oxygen retards corrosion by the promotion of a protective oxide film on the copper-nickel alloy surface, but increases the rate of corrosion by depolarizing cathodic sites and oxidizing cuprous ions to the more aggressive cupric ions. Other factors, such as velocity, temperature, salinity and depth affect dissolved oxygen transport and content in sea water thereby influencing the corrosion rate.

Soluble complexes of cuprous ($CuCl_2^-$, $CuCl_3^-$) and cupric ($CuCl^+$, $CuCl_2^\circ$, $CuCl_3^-$, $Cu(CO_3)_2^-$, etc.) ions are thermodynamically feasible in seawater. These complexes form at rates dependent upon the available concentration of Cu^+ and Cu^{++} ions. Complexation with organic ligands has been studied (Compton, 1973) and is hypothesized as a mechanism for the increased corrosivity of natural sea water over equivalent saline solutions. Organic complexation may be an important factor associated with biological activity and may be critical in biologically accelerated corrosion.

Polluted sea water has been cited (Gilbert, 1954) as the most important factor contributing to failure of copper alloy marine condenser tubes. The primary cause of accelerated attack of copper base alloys in polluted sea water is due to the presence of sulfide. The principal sources of sulfide in sea water are (1) the action of sulfate reducing bacteria, and (2) the putrefaction of organic sulfur compounds resulting in the formation of organic sulfides which can cause localized corrosion of copper nickel alloys in sea water (Bates and Popplewell, 1974).

Microbiological fouling of copper-nickel alloys in sea water and its influence on the corrosion process is not well-understood in comparison to the electrochemical processes. Corrosion scientists and engineers have studied the effects of organically derived sulfide and sulfur compounds, as previously mentioned, the effect of chlorination on corrosion (LaQue, 1950; Stewart and LaQue, 1952), and mechanical biofouling control methods with and without chlorination (Lewis, 1982). Sophisticated surface analytical techniques such as x-ray photoelectron spectroscopy (XPS) and scanning auger microscopy (SAM) have been utilized to study the development of inorganic and biological fouling layers on copper based alloys (Castle and Epler, 1981).

Most of these studies have been phenomenological, however, and have not adequately modelled the mechanisms of microbial attachment to copper-nickel surfaces and the role of microorganisms in the corrosion process. The following study is intended to identify some of the important aspects of microbial fouling and microbially-assisted corrosion of copper-nickel.

EXPERIMENTAL METHODS

Recycle Tubular Loop (RTL)

Three parallel recycle tubular loops (RTL) of the type shown in Figure 1 were used in this research. Pertinent dimensions and materials of construction are given in Table 1. A detailed description of the RTL system, analytical methods, and operation is presented elsewhere (Characklis and Zelver, 1983). Important features of the RTL include:

Each RTL is made predominantly of 0.625 in (0.0159 m) O.D. heat exchanger tubing with a wall thickness of 0.049 in (0.00124 m). Titanium or 70-30 copper-nickel tubing was used depending on the experimental design. A section of tubing is fitted with ports measuring *pressure drop*. A polyvinyl chloride shell encloses another section of to form a *heat exchanger* which is used to control bulk water temperature by excess heat build-up from pumping friction; a thermo-regulator detects when cooling is necessary and opens a solenoid valve to pass cold tap water over the section tubing. A *test section* comprised of 10 removable sections of tubing each 2 in (0.051 m) long is included for surface analyses of the deposit mass and the fouled surface (Figure 2).

A *flow meter* which measures cumulative water flow is used with a timer to calculate fluid flow velocity.

Water is recycled through the RTL by a *centrifugal* pump with a chemically resistant, phenolic head. Fluid flow rate is controlled manually by a ball valve located downstream of the flow meter.

A *pH* controller is not included but the buffering capacity of the aquarium salt maintains pH between 8.2 and 8.4.

A glass *mixing tank* is used for housing the thermo-regulator and for feed water input.

Feed Water Composition

Feed water consists of 11,300 mg ℓ^{-1} *aquarium salt* (Instant Ocean) for dilution to which one or more of the following may be added:

Trypticase Soy Broth (TSB) nutrition for microbial growth to give a nutrient loading rate (R_L) of either 0.92 or 9.2 mg m^{-2} min^{-1}.

Bacterial cells from a fixed film chemostat inoculated with *Pseudomonas atlanticus*, Flavobacterium, *Vibrio algenolyticus, Pseudomonas alcaligenes* and Desulfovibrio. The chemostat is continuously fed with 100 mg ℓ^{-1} Trypticase Soy Broth in 11,300 mg ℓ^{-1} salt water (Instant Ocean). Continuous analysis of chemostat output for a 7 month period shows $4.77 \times 10^9 \pm 8.20 \times 10^9$ total cells per hour and $3.37 \times 10^9 \pm 9.05 \times 10^9$ viable cells per hour.

Chlorine at a loading rate of 0.92 mg m^{-2} min^{-1} either continuously or periodically (one hour every 24 hours).

Filtration of the influent aquarium salt is used to minimize microorganisms in some experiments.

Analytical Methods

Analytical methods are described in detail elsewhere (Characklis and Zelver, 1983; Characklis *et al.*, 1982). Important features of these methods include:

Sampling for bulk water analysis is directly from the mixing tank using a sterile pipet. Surface samples are taken from the removable sample tubes by scraping the sample from the surface with a sterile rubber policeman into a beaker of sterile distilled water. All samples are homogenized with a high speed, sharp-bladed, mixer.

Total cell counts are measured by the AODC epifluorescence technique (Zimmerman and Meyer-Riel, 1974).

Viable cell counts are by the spread plate technique (APHA, 1976).

Deposit mass is measured by drying the removable sample tube for three hours at 100°C and then weighing the tube. The tube is then cleaned (deposit mass removed), dried and weighed again. The deposit mass is the difference between the dry fouled sample tube mass and the clean tube mass.

Corrosion rates are measured from the difference between mass of the sample tube at the experiment start and the cleaned sample tube at the experiment end. The difference in mass is divided by the exposure time to determine a rate which is then converted to units of microns per day.

Percent volatile deposit mass is determined on deposit mass scraped from the inside tube surface. Volatile mass is the mass removed by ignition at 600°C for one hour as described in Standard Methods (APHA, 1976).

Chemical analysis of the deposit mass was performed by atomic absorption.

Scanning Auger Microprobe (SAM) measurements were performed using the Phi 595 Model (Physical Electronics).

Chlorine was measured by the amperometric method.

RTL Operation

Table 2 presents a summary of conditions which were the same for all experiments. Conditions which varied include *tube alloy* (70-30 copper-nickel or titanium), *substrate loading rate* (0.92 or 9.2 mg TSB m^{-2} min^{-1}), and *treatment* (chlorination, filtration, or none).

RESULTS

Control Experiments

Experiments where no biocide has been added are referred to as control experiments. Controls have been conducted to observe the natural progression of fouling on the condenser tube surface. Figure 3 shows the progression of fouling for the titanium control experiments as indicated by change in Fouling Deposit Mass (M_D). Change in M_D for substrate loadings (R_L) of both 0.92 and 9.2 mg TSB m^{-2} min^{-1} are indicated. Note, the rate increase in M_D at R_L = 9.2 mg m^{-2} min^{-1} is approximately three times the fouling rate increase at R_L = 0.92 mg m^{-2} min^{-1}. The progression of M_D is indicated as linear since data are presently not available to justify a more sophisticated analysis. Presumably, as suggested by other work (Characklis, 1980), M_D reaches a plateau level at some point in time. However, for the initial stages of fouling, and for comparison, the linear regression analysis is sufficient.

Figure 4 shows the progression of M_D with time on copper-nickel tubing for the two substrate loadings. In this case, there is no significant difference between the substrate loadings.

Figure 5 shows the progression of fouling on copper-nickel and titanium tubing as indicated by change in Volatile Deposit Mass (M_{VD}). The rate increases in M_{VD} are calculated by multiplying the rate increases in M_D by the average percent volatile mass. At R_L = 0.92 mg m^{-2} min^{-1}, the rate increases in M_{VD} for copper-nickel and titanium show no significant difference. However, at R_L = 9.2 mg m^{-2} min^{-1}, M_{VD} accumulates approximately four times faster on the titanium surface compared to the copper-nickel surface.

Measurements of Corrosion Loss (C_L) for all control experiments are summarized in Table 3. C_L is zero on the titanium tubing and averages 33 microns per year for copper-nickel at R_L = 0.92

mg m^{-2} min^{-1}. Average C_L at the higher substrate loading (R_L = 9.2 mg m^{-2} min^{-1}) is approximately half that at the lower substrate loading.

Microbial Cell Counts

Total microbial cell counts on the copper-nickel and titanium surfaces, for all control experiments combined, show no significant difference between the two alloys (Figure 6). Table 4 summarizes all total and viable microbial cell counts taken for control copper-nickel and titanium experiments. No significant difference in cell counts between the two alloys is observed for measurements taken from either the tube surface or the bulk water.

Scanning Auger Microprobe Measurements

Scanning Auger Microprobe (SAM) measurements on sample tubes removed at the end of each experiment are summarized in Table 5. The values are weight percent of each element for the overall surface analyzed. Figure 7 shows the relationship between weight percent oxygen and the amount of volatile mass removed from the sample tube before the SAM measurement. Note, more oxygen is found on the metal surfaces containing greater attached volatile mass.

Chemical Analysis of Deposit Mass

An analysis of elements found within the deposit is presented in Table 6. Weight, percent of iron, and copper are measured on control copper-nickel sample and a control titanium sample. In addition, a sample of tygon tubing which connects copper-nickel tubing of the RTL to the glass tank, is analyzed to determine if any material from the copper-nickel is deposited elsewhere in the system. Results show considerably more copper in the deposit from the copper-nickel tube compared to the titanium (59 percent for CuNi versus 1.6 percent for the Ti). Weight percent iron changed little. A considerable amount of copper is found on the tygon section. Visual observation indicated a green tint to all deposits found in the RTL with copper-nickel tubing.

Filtration of Influent Water

In these experiments, the influent water is filtered and no substrate or bacteria is fed to the RTL. These experiments are designed to compare corrosion and fouling with and without bacteria. Contamination of the RTL occurred regardless of efforts to maintain aseptic conditions. However, the organism levels remain approximately an order of magnitude less on the "filtered" RTL surface compared to the control RTL (Table 7). Note, no difference in corrosion rate of the copper-nickel is observed between the filtered and control experiments.

Chlorination of Influent Water

Chlorine was added to the influent water at a loading rate of 9.2 mg m^{-2} min^{-1} both continuously and periodically for an hour every 24 hours. Figure 8 indicates the chlorine demand of the copper-nickel tubing. This experiment was conducted as a batch test to observe the reaction of chlorine with copper-nickel tubing. Free chlorine (20 mg ℓ^{-1}) was added to one liter of stirred solution. The amount of copper-nickel tubing added resulted in the same surface area to volume

ratio as in the RTL. Chlorine in the distilled water drops to approximately 13 mg ℓ^{-1} in the first 100 minutes and then remains constant. The chlorine exposed to the copper-nickel drops rapidly and, at 300 minutes, is no longer measurable. Combined chlorine in both solutions was always zero.

Table 8 compares results of the chlorine experiments to corresponding control experiments. The periodic chlorination of titanium is ineffective in reducing accumulation of deposit mass. However, continuous chlorination of titanium reduces M_D at 37 days from 22 g m^{-2} to 4.5 g m^{-2}. Surface cell numbers are reduced on the titanium surfaces exposed to both continuous and periodic chlorination. No significant difference in cell numbers is observed in the bulk water organisms. Only continuous chlorination is applied on the copper-nickel RTL. The results show no significant difference in deposit mass, corrosion rate, or in surface and bulk water organisms.

DISCUSSION

The results of this study do not justify the development of a new theory for microbially-mediated corrosion in Cu-Ni alloys. However, the results are useful for proposing a model to describe the process which may serve as a hypothesis for further experimentation.

A Conceptual Model for Microbially-Mediated Corrosion of Cu-Ni Alloys

The processes of major concern in this experimental system are corrosion of the metal surface and accumulation of fouling biofilm deposit. The processes occur simultaneously and interact with each other. Figure 9 is a schematic representation of the individual processes contributing to the corrosion and fouling processes. Table 9 identifies each of the processes designated by a number in Figure 9.

Initially, the metal surface is exposed to water containing substrate (an energy source for microbial growth), biomass (microbial cells), and dissolved oxygen. The corrosion process begins with the transport and reaction of oxygen at the metal surface (Process #1) which forms a protective oxide layer of insoluble corrosion products on the metal surface (Process #2). The events leading to corrosion of Cu-Ni alloys and the resulting composition of the surface oxide layer is complex and has been mentioned briefly in an earlier section. Random detachment and attachment of the insoluble corrosion products from the metal surface may occur due to the fluid motion and resulting shear stress (Processes #4 and #5). The detachment of insoluble corrosion products may initiate pit growth in the metal surface due to electrochemical corrosion (Process #3). Soluble corrosion products also diffuse into the bulk fluid (Process #13). The microbial cells (biomass) entering the system are suspended in the bulk fluid and consume substrate (Process #8) and dissolved oxygen (Process #9) resulting in cellular growth and reproduction. Some fraction of the suspended microorganisms attach to the metal surface (Process #11) and continue to consume substrate (Process #7) and dissolved oxygen (Process #10) resulting in growth and reproduction within the fouling deposit. The attached cells also produce extracellular polymers which further enhance attachment and adsorption of more cells, corrosion products, and other debris. The combined cellular and extracellular mass is termed the *biofilm*. A portion of the detached insoluble corrosion products become entrapped in the biofilm (Process #6). The biofilm continues to increase in density and thickness until fluid shear stress causes partial detachment (Process #12). Insoluble corrosion products may also detach with the biofilm (Process #12) thus leaving the metal surface more susceptible to corrosion processes. Soluble corrosion products are able to diffuse

directly out of the biofilm and enter the bulk fluid. After the biofilm has reached a certain thickness, anaerobic conditions form in the lower layers. These conditions are favorable for proliferation of sulfate-reducers which form sulfide and may lead to accelerated corrosion (Process #14).

A mathematical model has been developed to simulate this system and is presently being tested. The equations are an approximation of the processes occurring in the system. The initial calculations can serve to identify the dominant processes or rate-controlling processes. The results can be used to formulate hypotheses for experimental testing and for experimental design.

Influence of Substrate Loading Rate on Deposition

The accumulation of fouling deposit on a condenser tube surface is the net result of production and depletion processes. Prominent among the production processes are microbial metabolic processes and adsorption. Detachment or sloughing of deposit is perhaps the most important depletion process. Detachment may be quite important in explaining behavior in Cu-Ni alloys which are continuously releasing corrosion products into the bulk water.

An increase in substrate loading rate, R_L, significantly increased the amount of deposit accumulating on the titanium alloy as indicated in Figure 3. The volatile fraction of the deposit (organic component, including microbial cells, plus carbonates), however, decreased with increasing R_L (Table 3). The results suggest that at higher loading rates, dissolved oxygen was depleted in the lower layers of the biofilm and anaerobic microenvironments existed. Anaerobic metabolism generally results in a lower volatile solids content (Metcalf and Eddy, 1972).

R_L had no effect on total deposit accumulation on the Cu-Ni alloy (Figure 4). The volatile content of the deposit in the Cu-Ni was higher at the lower R_L as observed in the Ti alloy. The volatile deposit mass was significantly lower in the Cu-Ni as compared to the Ti tube at the high substrate loading (Figure 5). At low substrate loading, volatile deposit mass was essentially the same in both alloys. The relative ratio of volatile-to-total solids in the two alloys is predominantly influenced by the corrosion products observed in the Cu-Ni fouling deposits. The lower volatile deposit mass on the Cu-Ni is not easy to rationalize. One possibility is that the microorganisms' metabolism is altered by the Cu or Ni in the deposit, e.g., the organisms' extracellular polymer substance (EPS) production may be influenced by the presence of Cu.

The total and viable number of microbial cells in the deposit varied little between experiments or between alloys (Figure 6). These preliminary results suggest that Cu-Ni alloys are not very "toxic" to microorganisms (in contrast to macroorganisms). On the other hand, Cu-Ni may influence certain microbiological metabolic functions.

The results can be summarized as follows:

- Deposit mass increases with increasing R_L in the Ti alloy because more nutrients are available for microbial metabolism (Figure 3).
- Deposit mass in the Cu-Ni alloy does not increase with R_L (Figure 4) because much of the deposit consists of corrosion products as evidenced by the low deposit volatile fraction as compared to the Ti alloy.
- The change in deposit volatile fraction with different substrate loading rates may be due to increases in extracellular polymer substances (EPS) since cell numbers did not change.

- At higher R_L, dissolved oxygen may not penetrate the entire depth of the biofilm resulting in anaerobic microbial activity in the lower layers. Anaerobic biofilms generally exhibit lower volatile solids content (Metcalf and Eddy, 1972).

The hypothesis regarding oxygen is apparently contradicted by results of the Scanning Auger Microprobe (Table 5) which indicated elevated oxygen contents on the metal surface with increasing deposit mass (Figure 7). However, the oxide layer on the alloy most probably forms early in the experiment prior to biofilm formation. Consequently, the oxide layer may determine the amount of biofilm deposit which forms (Figure 7). Metal oxides vary in the degree to which they affect microbial processes and may not be nearly as active as the pure metal. Therefore, the oxidized Cu-Ni surface, although not "toxic," may provide an "inhospitable" surface for the microorganisms.

Increased R_L resulted in decreased corrosion rates in the Cu-Ni alloy (Table 3). However, the influence of R_L on corrosion is most probably an indirect effect. The influence of the deposit mass and its constituents (volatile mass and microorganisms) on corrosion, however, is probably more consequential and is discussed below.

Influence of Deposit Mass on Corrosion Rate of Cu-Ni

Increasing R_L has no effect on deposit mass in the Cu-Ni alloy but decreases the volatile content of the deposit. This is related to the fact that more corrosion occurs at low loading rates (Table 3) and a significant portion of the deposit consists of corrosion products (Table 6). Since total and viable cell numbers are relatively constant, several alternative hypotheses are advanced to explain the increased corrosion rate at low R_L:

- At low R_L, microbial cells produce more EPS (Trulear, 1982) and, thereby, increase the deposit volatile content although the deposit cell numbers remain relatively constant. The EPS, composed essentially of polyelectrolytes, acts as an electron source or sink to perpetuate or accelerate corrosion.

- At higher R_L, a significantly lower dissolved oxygen flux reaches the Cu-Ni surface (as a result of microbial activity) thus reducing corrosion rate.

- At higher R_L, metabolism of the deposit microorganisms changes in some other unknown manner resulting in decreased corrosion rate.

More experiments are necessary to reproduce and convincingly explain the increased corrosion rate of Cu-Ni at lower substrate loading rate. The precision and acccuracy of total and viable cell enumeration must be improved to quantitatively prove any mechanism. Experiments with monocultures or defined microbial communities may be necessary to improve such measurements.

Influence of Microbial Cell Numbers on Corrosion Rate of Cu-Ni

The experiment conducted with filtered sea water may help reduce the choices among hypotheses. The filtered sea water contained no microorganisms nor any trypticase soy broth (TSB) as a microbial energy source. Thus, any organisms in the system were contaminants and grew on chemical contaminants in the artificial seawater or dilution water. The result was a deposit

with dramatically lower viable cell counts and significantly lower total cell counts (Table 7). Despite the reduced number of microorganisms in the deposit, no difference in corrosion rate was observed. Several explanations for these observations are possible including the following:

- The number of microorganisms in the deposit does not influence corrosion rate.
- The dissolved oxygen concentration in the filtered experiment was much higher and increased corrosion rate enough to cancel any effect due to decreased level of microbial activity.
- The deposit organisms in the filtered experiment were significantly different from those in other experiments.
- The absence of organic substrate increased corrosion rate in the filtered experiment as much as microorganisms increased corrosion rate in the control experiments.

Detachment of the Fouling Deposit and Corrosion Rate in Cu-Ni

The model for microbially-mediated corrosion described above includes a term for detachment of fouling biofilm deposit from the tube surface. This process may influence corrosion rate substantially. When a portion (or a "patch") of deposit detaches, the metal surface left exposed will be subject to a considerably different microenvironment from the bare metal (i.e., metal surface with little or no deposit). As a consequence, a differential electrolytic cell may form increasing the potential for localized corrosion.

Chlorine Treatment and Corrosion of Cu-Ni Alloys

Chlorine is a very reactive compound and, hence, an effective bactericide. Chlorine is a strong oxidant which oxidizes many organic compounds and is known to depolymerize polymers of microbial origin (Characklis and Dydek, 1976). Therefore, chlorine has been used as an antimicrobial fouling treatment for many years. Recently, environmental concerns have encouraged searches for new, effective, yet environmentally safe, treatments. Nevertheless, chlorine is still widely used as a cooling water treatment.

Because of its reactive nature, chlorine treatment is frequently ineffective because it is consumed in undesirable side reactions, i.e., "chlorine demand" reactions. Usually, the chlorine demand is due to reduced inorganic compounds or organic compounds in the cooling water. However, Cu-Ni alloys also present a chlorine demand.

This study was conducted in artificial sea water. When chlorine is added to sea water containing bromide ion, the bromide is rapidly oxidized to bromine and the chlorine reduced to chloride. The chemistry of the reaction has been described elsewhere. As a result, and because no distinction was made between chlorine and bromine in our measurements, the combined chlorine and bromine will be referred to as "halogen" below.

Halogen demand. Figure 8 presents data from a halogen demand experiment. The results clearly indicate a high halogen demand for the Cu-Ni tube section. A halogen residual was never observed in the chlorination experiments as a result of the halogen demand presented by the metal tube, the sea water, and the trypticase soy broth.

Influence of halogen on deposit mass. Halogen treatment, in general, reduced deposit accumulation. The more dramatic effect was observed in the Ti tubes. Halogen treatment had little effect on deposit mass in the Cu-Ni tube nor did it influence microbial cell counts in the deposit or in the bulk water. The high halogen demand of the Cu-Ni tube surface area, TSB, and the artificial sea water resulted in no measurable halogen residual and, hence, partially explains the negligible effect of halogen on the accumulation of fouling deposit.

In the Ti tubes, the influence of halogen on total deposit mass was much more dramatic for at least two reasons:

1. The deposit mass in the Ti tubes contained significantly greater amounts of volatile components, i.e., microbial mass.
2. The Ti tube had little, if any, halogen demand.

Total and viable cell numbers in the deposit as well as in the bulk water were reduced significantly in the Ti system as a result of halogen treatment. The lack of halogen demand at the tube surface may influence the bactericidal nature of the halogen as compared to its effect in the Cu-Ni system. However, the influence of the Cu-Ni corrosion products trapped in the deposit may have also influenced the reactivity of the halogen.

Influence of halogen treatment on corrosion rate in Cu-Ni. Table 8 indicates no significant effect of halogen treatment on corrosion rate of Cu-Ni. If halogen had significant contact with the Cu-Ni surface, considerable corrosion would be expected due to its high halogen demand. Since no significant corrosion was observed, chlorine may have been consumed in undesirable side reactions and may not have been penetrating the fouling deposit to the Cu-Ni surface. Additionally, Cu-Ni may serve as a catalyst for halogen reduction and, if so, little corrosion would occur as a result of a halogen reduction. More experiments are necessary to determine if a higher halogen loading rate would reduce fouling but, at the same time, increase corrosion rate.

Limitations of the Study

This study was conducted in the laboratory in order to control environmental conditions and to isolate the various processes which influence fouling and corrosion. Consequently, there are several factors which must be considered in interpreting these data or extrapolating the results for field applications. The following limitations were apparent during the investigation and serve as starting points for further experimentation:

- The microbial population was an undefined mixed culture. Changes in dominant species undoubtedly occurred between experiments in which environmental variables were adjusted. The specific influence of a specific organism on fouling and corrosion is unknown except for some few instances.

- The corrosion loss measurements and SAM results quoted represent values over the tube surface. The average values are not a true representation of the corrosion process and, generally, underestimate the potential damage from pitting or crevice corrosion. Pits were observed and were analyzed in more detail elsewhere (Characklis and Zelver, 1983).

- Artificial sea water was used. The problems associated with its use, if any, are not clearly documented.

- The substrate used for microbial growth, TSB, is not representative of all waters. Nevertheless, TSB is a diverse mixture of organic compounds, many of which are found in natural environments. The concentrations used are representative of natural waters.

- The time of exposure for the Cu-Ni tubes was short compared to its projected lifetime in a condenser or other applications. The ultimate effect of fouling and corrosion over a long period due to our experimental manipulations is unknown.

- Sampling of the deposit mass required procedures which may have disturbed or influenced the total amoung of oxide layer or other corrosion products residing on the tube surface after deposit removal.

SUMMARY

A conceptual model has been proposed to describe the interrelationship between biofouling and corrosion in a Cu-Ni alloy. Laboratory results have been presented which are consistent with the proposed model. The experimental results suggest several mechanistic hypotheses requiring further experimental testing which is currently underway.

ACKNOWLEDGMENTS

The authors gratefully acknowledge the National Science Foundation (CPE 80-17439), Office of Naval Research (N 00014-80-C-0475), Calgon Corporation, and Montana State University Engineering Experiment Station for partial financial support; the NSF Regional Instrumentation User Facility (NSF-CHE-7916 134) Center for Research in Surface Science and Submicron analysis (CRISS) located at Montana State University for use of the Scanning Auger Microprobe (SAM); G. J. Lapeyre, J. R. Anderson, D. J. Frankel and M. C. Jaehnig at CRISS for their valuable and kind assistance in using and interpreting SAM results; and Tico Titanium, Olin Fineweld Tube, and Wolverine Division for supplying heat transfer tubing.

REFERENCES

APHA Standard Methods for the Examination of Water and Wastewater, 14th Edition, APHA, Washington, DC, 1976.

Bates, J. F., Popplewell, J. M. Corrosion of Condenser Tube Alloys in Sulfide Contaminated Brine, Paper No. 100 presented NACE Corrosion/74, Chicago, IL, March 1974.

Bianchi, G., Longhi, P. Corrosion Science, Vol. 13, p. 853 (1973).

Bongers, L. H., O'Conner, T. P. Bromine Chloride–An Alternative to Chlorine for Fouling Control in Condenser Cooling Systems. Prepared for U.S. Environmental Protection Agency, 7-77-053, May 1977.

Bryers, J., Characklis, W. G. Water Research, Vol. 15, p. 483 (1981).

Castle, J. E., Epler, D. C. The Development of Inorganic and Biological Fouling Layers on Copper Based Alloys, paper presented at the Ist. Corrosion Science TECHNOL/Inst. Chemical

Engineering Conference on Progress in the Prevention of Fouling in Industrial Plant, Univ.. of Nottingham, UK, April 1981.

Characklis, W. G., Nimmons, M. J., Picologlou, B. F. Journal of Heat Transfer Engineering, Vol. 3, p. 23 (1981).

Characklis, W. G. Biofilm Development and Destruction, Electric Power Institute, Final Report, CS-1554, Project 902-1, September 1980.

Characklis, W. G., Zelver, N. Biofilm Development and Control in Simulated Shipboard Condenser Tubes. Preliminary report for the David Taylor Naval Ship Research and Development Center, 1983.

Characklis, W. G., Bryers, J. D., Trulear, M. G., Zelver, N. Water Research, Vol. 16, p. 1207 (1982).

Characklis, W. G., Dydek, S. T. Water Research, Vol. 10, p. 515 (1976).

Compton, K. G. Corrosion Reactions in Natural Sea Water as Compared to Reactions in Various Synthetic Saline Corrosive Media, Paper No. 9 presented NACE Corrosion/73, Anaheim, CA, March 1973.

Corpe, W. A. Microfouling: The Role of Primary Film-Forming Marine Bacteria, Proc. 3rd Int'l Congress on Marine Corrosion and Fouling, Northwestern Univ., Evanston, IL, p. 598, 1973.

DePalma, V. A., King, R. W., Fornalik, M., Meyer, A. E., Baier, R. E. Analysis of Primary Films Accumulated During Marine Fouling Program. Prepared for David W. Taylor Naval Ship R&D Center, Annapolis, MD, Contract No. N00167-80-C-0178, Arvin Calspan, Buffalo, NY, October 1981.

DePalma, V. A., Goupil, D. W., Akers, C. K. Field Demonstration of Rapid Microfouling in Model Heat Exchanger: Gulf of Mexico, November 1978, presented at 6th OTEC Conference, Washington, DC, 1979.

Dexter, S. C. Microbiological Fouling and Its Control in Coastal Water and the Deep Ocean, Woods Hole Oceanographic Institution Report No. WHOI-74-64, September 1974.

Efird, K. D., Anderson, D. B. Materials Performance, Vol. 14, No. 11 (1975).

Efird, K. D. The Interrelation of Corrosion and Fouling of Metals in Sea Water, paper presented NACE Corrosion/75, Toronto, April 1975.

Gilbert, P. T. Trans. Inst. of Marine Engineers, Vol. 66, No. 1 (1954).

Huguenin, J. E., Ansuini, F. J. The Design, Construction, Testing and Evaluation of Copper Based Ccommercial Prototype Equipment for Use in Marine Aquaculture, International Copper Research Association, Inc. technical paper, New York, NY, January 1980.

LaQue, F. L. Discussion of paper, Corrosion, Vol. 6, No. 4 (1950).

Lewis, R. O. Materials Performance, Vol. 21, No. 9 (1982).

Loeb, G., Neihof, R. Adv. Chem. Series, No. 145, American Chemical Society, p. 319 (1973).

Marine Research. A Report on Possible Alternatives to Chlorination for Controlling Fouling Power Station Cooling Water Systems, Marine Research, Inc., Falmouth, MA, April 1976.

Metcalf and Eddy. Wastewater Engineering, McGraw-Hill, Inc. (1972).

North, R. F., Pryor, M. J. Corrosion Science, Vol. 10, p. 297 (1970).

Nosetani, T., Sato, S., Onda, K., Kashiwada, J. Effect of Marine Biofouling on the Heat Transfer Performance of Titanium Condenser Tubes, Suitomo Light Metal Industries Ltd., Technical Research Laboratories, June 1979.

Picologlou, B. F., Zelver, N., Characklis, W. G. Journal of the Hydraulics Division, ASCE, Vol. 106, No. HY5, Proc. Paper 15421, p. 733 (1980).

Ritter, R. B., Suitor, J. W. Fouling Research on Copper and Its Alloys—Seawater Studies, International Copper Research Association, Inc. technical paper, April 1976.

Sechler, G. E., Gundersen, K. Role of Surface Chemical Composition on the Microbial Contribution to Primary Films, Proc., 3rd Int. Congress on Marine Corrosion and Biofouling, October 1972, Nat. Bureau of Standards, Gaithersburg, MD.

Stewart, W. C., LaQue, F. L. Corrosion, Vol. 8, No. 8 (1952).

Tracor Marine. Final Report: Ocean Thermal Energy Conversion (OTEC) Biofouling and Corrosion Experiment 1978 St. Croix, U.S. Virgin Islands, Project Summary, Part I of a three-part report, submitted to: Pacific Northwest Laboratory, Richland, Washington, for the U.S. Department of Energy, Job No. 713804, UC-64, PNL-2739.

Trulear, M. B. Cellular Reproduction and Extracellular Polymer Formation in the Development of Biofilms, a thesis draft submitted for Doctor of Philosophy, Dept. of Civil Engineering, Montana State University, 1982.

Zimmerman, R., Meyer-Reil. Kiel Meeresforsch, Vol. 30, p. 24 (1974).

Table 1. Pertinent Dimensions and Construction Materials of the Recycle Tubular Loop

Liquid Volumes		V (m^3)	
Tubing (CuNi or Ti, PVC and Tygon)		0.00095	
Centrifugal Pump (phenolic)		0.00018	
Flow Meter (PVC)		0.00024	
Mixing Tank (glass)		0.00035	
	Total Volume	0.00172	
Tubing Lengths and Inside Diameters		L (m)	ID (m)
Heat Exchanger (CuNi or Ti)		0.76	0.0134
Pressure Drop Section (CuNi or Ti)		1.22	0.0134
Test Section (CuNi or Ti): 10 0.051 μm long sample tubes		0.51	0.0134
Connecting Tubing (CuNi or Ti)		1.21	0.0134
	Total Length of Metal Tubing	3.70	
Connecting Tubing (Tygon)		0.16	0.0159
Connecting Tubing (PVC)		1.30	0.0175
	Total Length	5.16	
Surface Area		m^2	
	Total Area	0.1033	

Table 2. Summary of Conditions which were Identical for All Experiments

Volumetric Feed Rate	1.9×10^{-5} (m^3 min^{-1})
Hydraulic Retention Time	90 (min)
Water Temperature	30 (°C)
pH	8.2 - 8.4
Fluid Flow Velocity	54 (m min^{-1})
Fluid Shear Stress	3.0 (N m^{-2})
Salt Concentration	11,300 (mg ℓ^{-1})

Table 3. Corrosion Loss and Volatile Deposit Mass for All Control Copper-Nickel and Titanium Experiments

Alloy	Substrate Loading (mg m^{-2} min^{-1})	Corrosion* Loss (μm yr^{-1})	Volatile* Deposit Mass (percent)
CuNi	0.92	33 ± 6(14)	28 ± 9(5)
Ti	0.92	0 ± 0(2)	76 ± 9(2)
CuNi	9.2	16 ± 9(4)	13(1)
Ti	9.2	—	28 ± 11(2)

*Values given are mean ± one standard deviation with the # of samples given in parentheses.

Table 4. Viable and Total Cell Counts in the Bulk Water and in the Deposit Mass for All Control Copper-Nickel and Titanium Experiments

Sample (alloy)	Bulk Water Cells (10^8 cells hr^{-1})†		Attached Cells (10^8 cells cm^{-2})	
	STP*	EPI**	STP*	EPI**
CuNi	2.0 ± 2.2(26)	4.4 ± 4.3(28)	0.4 ± 0.32(5)	1.1 ± 0.8(13)
Ti	1.6 ± 1.6(12)	4.0 ± 6.1(16)	3.9 ± 6.9(4)	2.2 ± 1.2(7)

Note. Values given are the mean ± one standard deviation with the number of samples given in parentheses.
*STP: standard plate count (viable cells)
**EPI: AODC by epifluorescence (total cells)
†Number of cells exiting the reactor per hour in the bulk water flow

Table 5. Scanning Auger Microprobe Analyses of Elements on Copper-Nickel Surface After Removal of Fouling Deposit Mass

	Cu	Ni	Fe	Mn	O	N	Ca	C	Cl	S
Control	49.7	34.4	2.4	0.7	8.4	0.3	0.4	1.1	2.4	0.6
Filtered	43.8	34.5	0.8	1.8	10.7	0.4	0.5	2.8	3.3	0.3
Chlorinated	75.0	12.3	2.1	1.1	5.2	0.2	0.6	1.4	1.1	0.3
New CuNi	67.6	26.5	1.2	1.6	0.9	0.4	0.6	1.0	2.7	0.5

Table 6. Atomic Absorption Analyses of Iron and Copper Within the Fouling Deposit Mass

Sample	Exposure Time (days)	Condition	Percent of Total Deposit Mass	
			Iron	Copper
CuNi	22	Control	1.21	59.12
Tygon	22	Control	0.40	31.80
Ti	23	Control	3.88	1.58

Table 7. Fouling Deposit Mass, Corrosion Loss, Percent Volatile, Deposit Mass and Microbial Analysis of Deposit for Control and Filtered Experiments

Sample (alloy)	Exposure Time (days)	Condition	Deposit Mass ($g\ m^{-2}$)	Corrosion Loss ($\mu m\ yr^{-1}$)	Volatile Deposit (%)	Cells in Deposit	
						STP* (10^3 cells cm^{-2})	EPI** (10^7 cells cm^{-2})
CuNi	45	filtered	7.5±4.2(33)	14±11(4)	53	1.3(1)	0.32±0.02(5)
CuNi	45	control	12.4±6.1(3)	16±9(4)	13	8.0(1)	8.6 ±1.6(5)
Ti	37	filtered	2.0±3(8)	—	—	9.3(1)	2.5 ±7.0(5)
Ti	37	control	22.1±1.2(8)	—	36	—	1.5 ±5.0(5)

Note. Values given are the mean ± one standard deviation with the number of samples given in parentheses.
*STP: standard plate count (viable cells)
**EPI: AODC by epifluorescence (total cells)

Table 8. Fouling Deposit Mass, Corrosion Loss, Percent Volatile Deposit Mass and Microbial Analyses for Control and Chlorine Experiments

Sample (alloy)	Exposure Time (days)	Condition	Deposit Mass ($g\ m^{-2}$)	Volatile Deposit Mass (%)	Corrosion Loss ($\mu m\ yr^{-1}$)	Deposit Cells (10^6 cells cm^{-2})		Bulk Water Cells (10^6 cells cm^{-3})	
						STP*	EPI**	STP*	EPI**
Ti	10	control	3.3±1.4(2)	—	—	6.1±5.4(2)	118±59(2)	6.3 ±2.3(2)	30 ±17(2)
Ti	10	5 mg ℓ^{-1} cl_2 (periodic for 1 hr each 24 hr)	5.0±0.5(2)	—	—	62 ±75(2)	168±185(2)	8.4 ±.8(2)	39 ±6.3(2)
CuNi	45	5 mg ℓ^{-1} cl_2 (continuous)	10.0±6.4(3)	10(1)	13±10(4)	85(1)	17(1)	0.96±.61(5)	3.2±1.3(10)
CuNi	45	control	12.4±6.1(3)	13(1)	16±9(4)	80(1)	86(1)	2.7 ±2.0(5)	6.3±4.3(10)
Ti	37	5 mg ℓ^{-1} cl_2 (continuous)	4.5±1.3(8)	—	—	0.10(1)	6.2(1)	0.37±.39(4)	4.0±3.2(7)
Ti	37	control	22.1±1.2(8)	—	—	—	150(1)	0.90±0.50(4)	3.6±1.5(7)

Note. Values given are the mean ± one standard deviation with the number of samples given in parentheses.
*STP: standard plate count (viable cells)
**EPI: AODC by epifluorescence (total cells)

Table 9. Explanation of Process Terms Used in Corrosion Model

1) Dissolved oyxgen removal by metal surface
2) Corrosion product formation
3) Soluble corrosion product detachment from metal surface
4) Insoluble corrosion product detachment from metal surface
5) Insoluble corrosion product attachment to metal surface
6) Insoluble corrosion product attachment to biofilm
7) Substrate removal by biofilm
8) Substrate removal by suspended biomass
9) Dissolved oxygen removal by suspended biomass
10) Dissolved oxygen removal by biofilm
11) Suspended biomass attachment to biofilm
12) Biofilm and insoluble corrosion product detachment from metal surface
13) Soluble corrosion product diffusion through biofilm
14) Anaerobic corrosion product formation

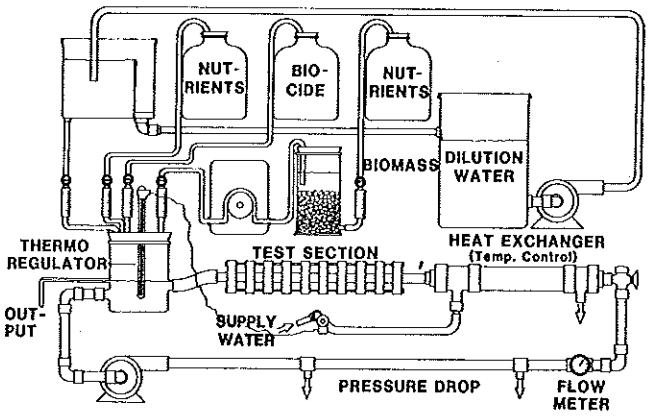

Figure 1. Schematic of Recycle Tubular Loop

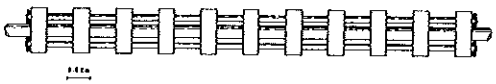

Figure 2. Recycle Tubular Loop Test Section

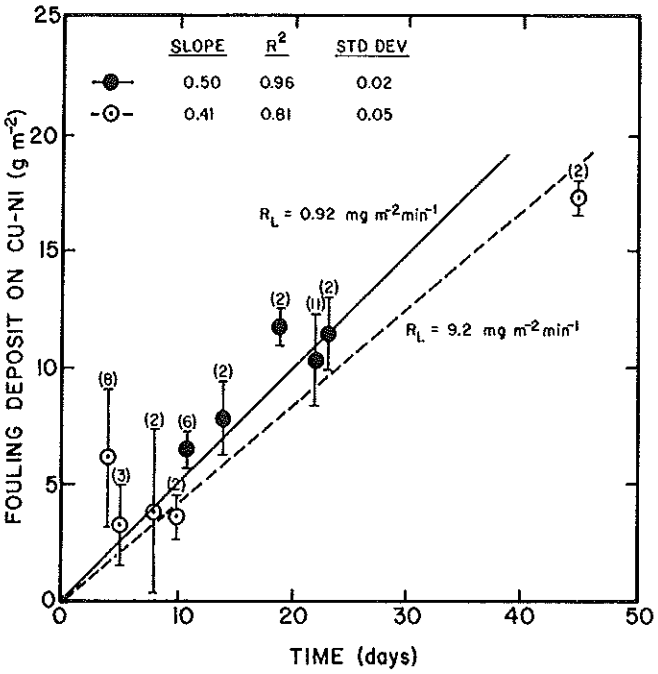

Figure 4. Progression of Fouling Deposit Mass with Time on Copper-Nickel (slope regression fit forced through zero)

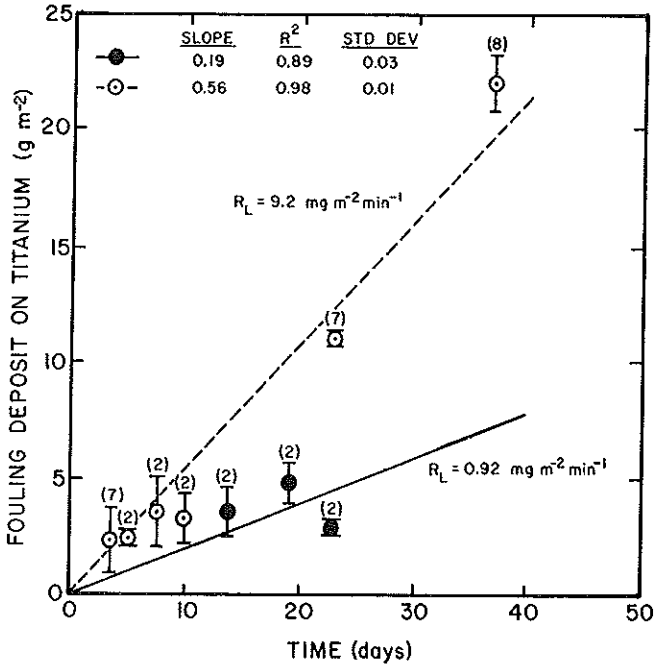

Figure 3. Progression of Fouling Deposit Mass with Time on Titanium (slope regression fit forced through zero)

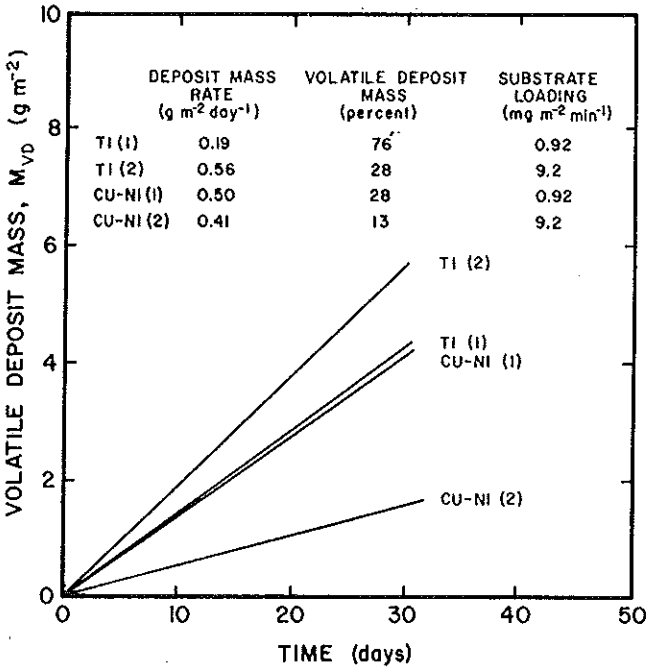

Figure 5. Progression of Volatile Fouling Deposit Mass with Time on Copper-Nickel and Titanium

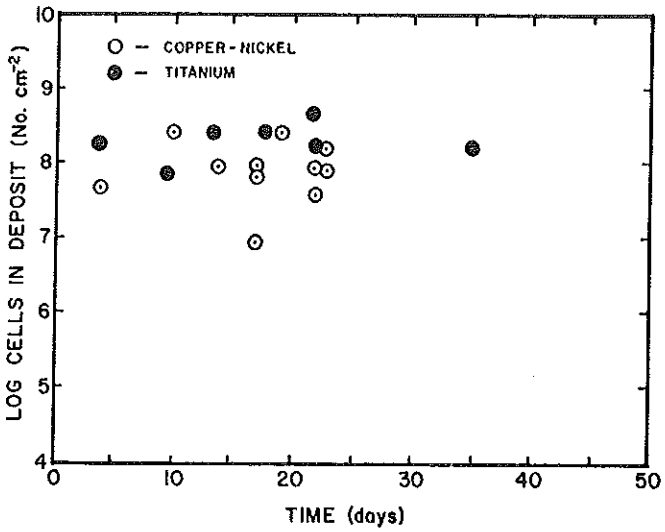

Figure 6. Total Microbial Cells Within Deposit for All Control Copper-Nickel and Titanium Experiments

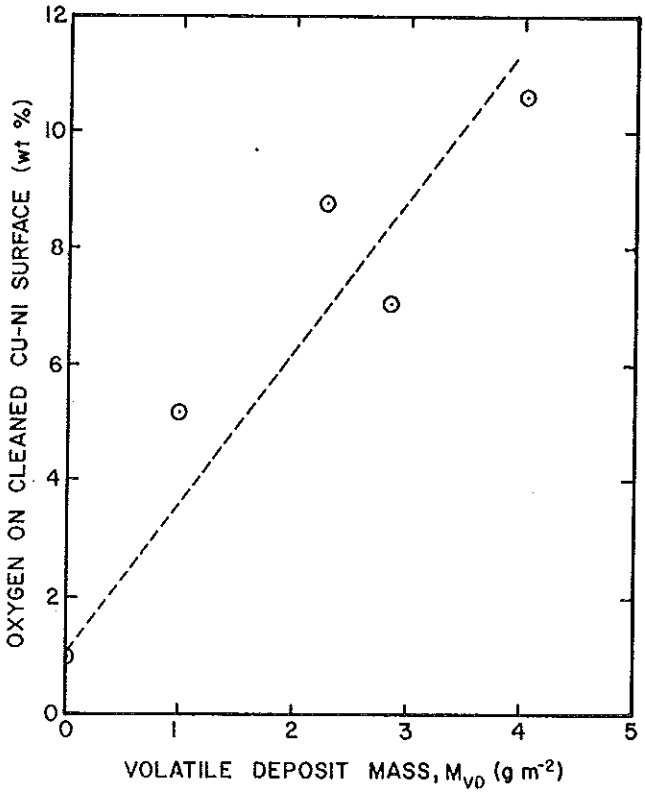

Figure 7. Weight Percent Oxygen on Copper-Nickel versus Fouling Deposit Removed

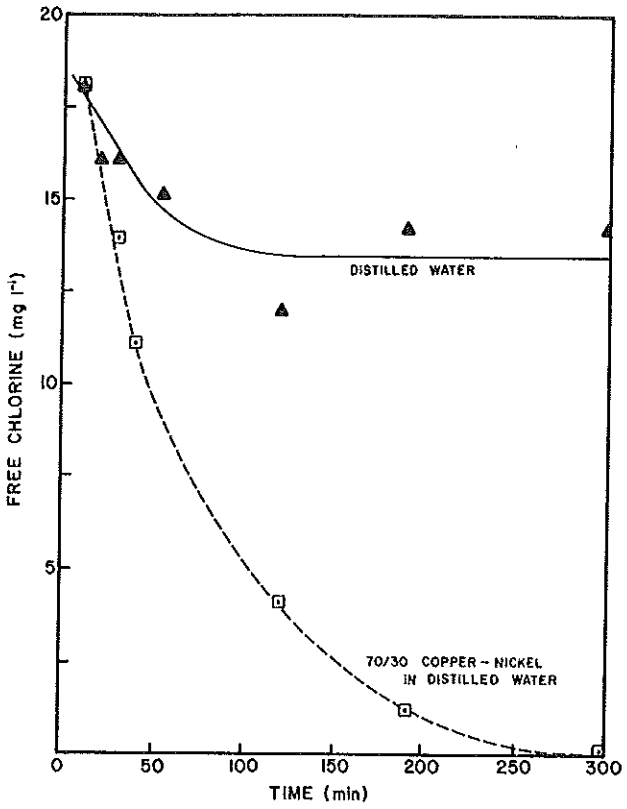

Figure 8. Free Chlorine versus Time for One Liter Distilled Water With and Without Submerged Copper-Nickel Samples

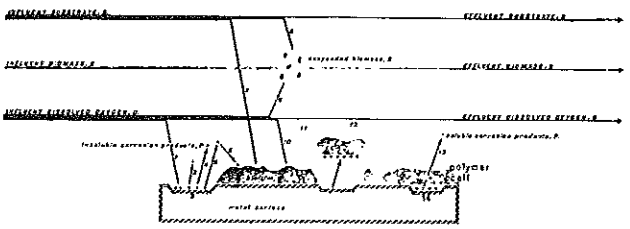

Figure 9. Schematic Representation of Individual Process Contributing to the Corrosion and Fouling Processes